Volume 1 | Number 1 | Jan 2013 | Pages 1–100

Chemical Science

www.rsc.org/chemicalscience

This is an *Accepted Manuscript*, which has been through the Royal Society of Chemistry peer review process and has been accepted for publication.

Accepted Manuscripts are published online shortly after acceptance, before technical editing, formatting and proof reading. Using this free service, authors can make their results available to the community, in citable form, before we publish the edited article. We will replace this *Accepted Manuscript* with the edited and formatted *Advance Article* as soon as it is available.

You can find more information about *Accepted Manuscripts* in the **Information for Authors**.

Chemical Science

ARTICLE

Entropy Driven Chain Effects on Ligation Chemistry

Kai Pahnke,[ab] Josef Brandt,[cd] Ganna Gryn'ova,[e] Peter Lindner,[f] Ralf Schweins,[f] Friedrich Georg Schmidt,[g] Albena Lederer,*[cd] Michelle L. Coote,*[e] Christopher Barner-Kowollik*[ab]

We report the investigation of fundamental entropic chain effects that enable the tuning of modular ligation chemistry – for example dynamic Diels–Alder (DA) reactions in materials applications – not only classically *via* the chemistry of the applied reaction sites, but also *via* the physical and sterical properties of the molecules that are being joined. Having a substantial impact on the reaction equilibrium of the reversible ligation chemistry, these effects are important when transferring reactions from small molecule studies to larger or other entropically very dissimilar systems. The effects on the DA equilibrium and thus the temperature dependent degree of debonding (%$_{debond}$) of different cyclopentadienyl (di-)functional poly(meth-)acrylate backbones (poly(methyl methacrylate), poly(*iso*-butyl methacrylate), poly(*tert*-butyl methacrylate), poly(*iso*-butyl acrylate), poly(*n*-butyl acrylate), poly(*tert*-butyl acrylate), poly(methyl acrylate) and poly(isobornyl acrylate)), linked *via* a difunctional cyanodithioester (CDTE) were examined *via* high temperature (HT) NMR spectroscopy as well as temperature dependent (TD) SEC measurements. A significant impact of not only chain mass and length with a difference in the degree of debonding of up to 30 % for different lengths of macromonomers of the same polymer type but – remarkably – as well the chain stiffness with a difference in bonding degrees of nearly 20 % for isomeric poly(butyl acrylates) is found. The results were predicted, reproduced and interpreted *via* quantum chemical calculations, leading to a better understanding of the underlying entropic principles.

Introduction

The Diels–Alder (DA) cycloaddition is long known and – especially after the introduction of the click chemistry concept by Sharpless and colleagues in 2001 – widely used due to its synthetic benefits such as readily accessible starting materials, facile handling, the lack of side products and in some cases quantitative conversion.[1,2] Consequently, DA reactions are employed in great variety in applications ranging from molecular conjugation, total synthesis, block copolymer formation, dendrimers to thermoreversible ligation and surface modification, as well as surface patterning to name only a few.[3-13] To enable such a wide field of applications, several hetero Diels–Alder (HDA) pairings such as cyclopentadiene (Cp) with different dithioester, thioaldehyde or nitrosocarbonyl functionalities have been explored to allow catalyst free reactions at ambient temperature and mild retro Diels–Alder (rDA) adduct cleavage temperatures.[4,14-16] Based on their thermoreversible character, DA reactions have gained importance in the field of self-healing materials.[17-22] These smart materials allow a change from passive to tailor-made responsive materials upon a given stimulus *via* extrinsic healing mechanisms as, for instance, the release of a healing agent or intrinsic ones with the aid of integrated reversible bonds to

prevent material failure.[19,23] Extrinsically self-healing materials are most commonly generated *via* the incorporation of fibers or microcapsules filled with healing agents, for example cross-linkable monomers, catalysts or multilinkers in concrete or epoxy resins, which are released upon material damage and allow the formation of a network and prevent crack propagation while maintaining the material properties.[20,24,25] While materials with extrinsic self-healing properties can only undergo a finite number of healing cycles due to the limited amount of incorporated healing agent, intrinsic ones – in theory – enable unlimited healing as the broken covalent bonds can be reformed. To achieve intrinsic self-healing, reversible bonds such as supramolecular interactions, photo-induced metathesis or thermoreversible reactions have to be integrated in the material chemistry itself. As covalent bonds give rise to higher material strengths than non-covalent interactions, and as the temperatures needed for the reversal of the DA reactions lie in an easily accessible, yet sufficiently high range for many materials applications, more and more self-healing materials with variable DA chemistry are under investigation.[19]

Classically, the DA equilibrium and the associated opening or closing temperature of its adducts is tuned *via* the chemistry of the employed diene and dienophile functional groups and

therefore their reaction enthalpy. Different electron withdrawing or donating substituents generate favorable HOMO-LUMO interactions; the application of advantageous geometries such as cyclic and thus pre-oriented dienes or the use of Lewis acids as catalysts in HDA reactions allow the adjustment of these parameters and thus also the modification of the material properties.[4,11,14,17,26-29] In 2013, Barner-Kowollik and colleagues observed, in accordance with Gibbs equation ($\Delta G = \Delta H - T\Delta S$), that not only chemical factors are able to significantly affect these characteristics, but also entropic ones, thereby providing a likely explanation for the differences in published debonding temperatures of otherwise identical DA systems.[17,30,31] It could be predicted in theory and shown in multiple experiments that the chain length and mass of the moieties which are linked *via* DA chemistry are able to drastically influence the reaction equilibrium between open reaction sites and closed adducts.[32] This behavior arises from the different mass and length specific contributions of translational and rotational entropy, which are released during chain scission events and hence the more or less favorable release of the incorporated building blocks. Such effects can be purposely used to further alter the properties and processing parameters of intrinsically self-healing materials such as cross-linked DA networks *via* their mesh size. Moreover, entropic effects also have to be considered when conjugation techniques are transferred from small model systems to polymer chains with considerably different entropic characteristics, as the previously expected behavior may be severely altered by the difference in entropy of the connected species.

Given the crucial role that entropy plays in determining the temperature dependent degree of debonding, an obvious question is to what extent do other physical or chemical factors than molecular mass and length including chain stiffness in general, or side chain substituents in particular, influence the equilibrium position through their effects on rotational, translational and vibrational entropy. To address this question, a set of experiments including temperature dependent characterization with ten polymeric building blocks based on eight (meth-) acrylate monomers with sterically different side-chain groups was designed.[33] Thereby, not only diverse masses (**Scheme 1 (a)**), but also connected units of varying stiffness can be studied, as the different degrees of steric hindrance depend on the side chain substituents and lead to differing chain mobility and thus stiffness values (**Scheme 1 (b)**).[34] Evidencing the effects on polymers featuring thermolabile connection units should be understood in a model sense, enabling the alteration of the molecular characteristics under investigation in a facile way. Clearly, the principle operation of entropic effects is as well valid for all other reversible connection points including supramolecular ones and not limited to synthetic polymers. A,A'-Diblock polymers connected by DA chemistry using building blocks of the same length, yet differing in either chain stiffness or mass, were synthesized and their temperature dependent debonding behavior was characterized *via* high temperature nuclear magnetic resonance spectroscopy (HT NMR) (**Scheme 1 (i)**). To widen the view and systematically clarify the observed effects, DA polymers consisting of isomeric difunctional building blocks of again the same length and also mass with different chain stiffness were examined and characterized *via* HT NMR and temperature dependent size exclusion chromatography (TD SEC) (**Scheme 1 (ii)**). Finally, the chain length dependent specificity of the newly observed chain stiffness effect was studied *via* the evaluation of DA polymers based on two building block pairs of the same basic chain segment mobility, but different lengths and thus also masses (**Scheme 1 (iii)**). The experimental observations are compared with the results of quantum chemical calculations to explain the source of the effects *via* their underlying entropic principles.
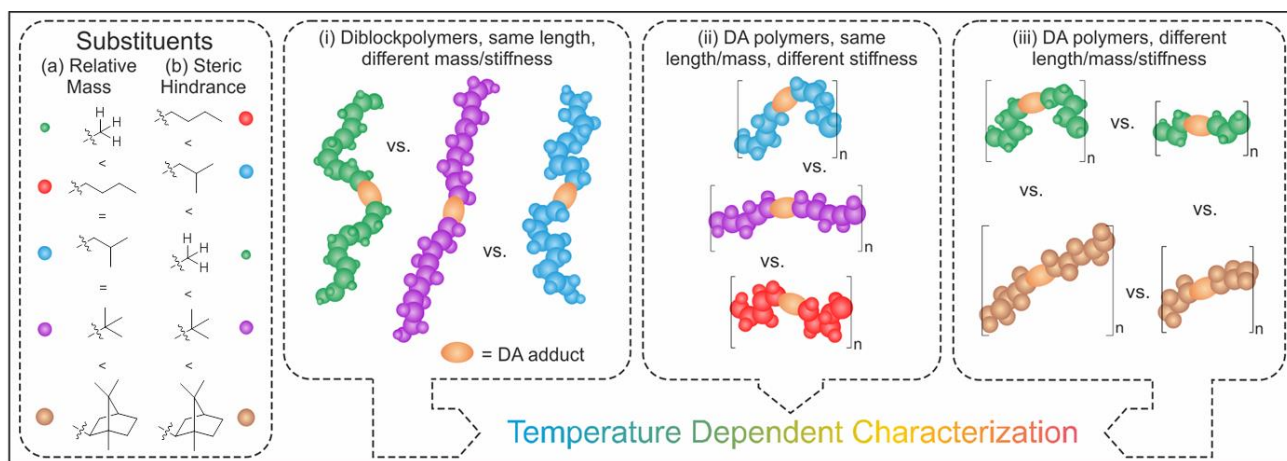
Scheme 1 The examined side chain substituents with a comparison of (a) their relative masses and (b) the assumed impact of their steric hindrance on chain movement as well as approaches to investigate the chain mass, length and stiffness effect of polymer building blocks on their ligation chemistry *via* HT NMR and TD SEC characterization: (i) A,A'-diblockpolymers consisting of building blocks of the same length yet different mass or stiffness, (ii) DA polymers based on building blocks of the same length and mass, but different stiffness and (iii) DA polymers with different building block sizes and chain stiffness.

Experimental Section

Materials. Stabilized methyl acrylate, *iso*-butyl acrylate (Alfa Aesar, 99 %), isobornyl acrylate (ABCR, 85 %), *tert*-butyl

methacrylate (Sigma-Aldrich, 98 %), *iso*-butyl methacrylate, methyl methacrylate (ABCR, 99 %), *tert*-butyl acrylate and butyl acrylate (Sigma-Aldrich, 99 %) were deinhibited *via* a short column of basic aluminum oxide. Copper(I) iodide (Sigma-Aldrich, ≥ 98 %), tin(II) 2-ethylhexanoate (Sigma-Aldrich, 95 %), tris[2-(dimethylamino)ethyl]amine (Sigma-Aldrich, 97 %), butylene bis(2-bromoisobutyrate) (provided by Evonik), ethyl α-bromoisobutyrate (Sigma Aldrich, 98 %), anisole (Acros, 99 %), methanol (VWR, p.a.), triphenylphosphine and sodium iodide (ABCR, 99 %) were used as received. Tetrahydrofurane (Sigma-Aldrich, anhydrous, ≥ 99.9 %) and nickelocene (ABCR, 99 %) were used as received and handled in a glovebox.

Synthesis of a Cyanodithioester Dilinker. The synthesis was conducted according to literature.[14] The cyanodithioester (CDTE) dilinker (**Scheme 3**) was obtained as a yellow solid. Overall yield: 5 %. ^{1}H NMR (400 MHz, CDCl$_3$) δ [ppm]: 7.41-7.29 (m, 8H, Ar*H*), 7.22-7.20 (m, 1H, N*H*), 6.65-6.63 (dd, J = 5.4, 2.8 Hz, 1H, C=C*H*), 6.45-6.43 (dd, J = 5.1, 2.8 Hz, 1H, C=C*H*), 6.10-6.08 (dd, 5.2, 3.3 Hz, 1H, C=C*H*), 5.80-5.78 (dd, 5.2, 3.3 Hz, 1H, C=C*H*), 5.12-5.04 (m, 4H, NCOOC*H$_2$*), 4.82 (s, 1H, C*H*SC), 4.54 (s, 1H, C*H*SC), 4.30-4.071 (m, 4H, SC*H$_2$*Ar), 4.01-3.98 (m, 2H, C*H*CCN), 3.81 (br, 1H, OCONHC*H*), 2.97-2.87 (br, 2H, OCONHC*H$_2$*), 2.15-1.82 (m, 4H, CHC*H$_2$*CH), 1.75-1.69 (br, 2H, CH$_2$), 1.23-0.80 (m, 13H, C*H$_3$*, C*H$_2$*).

Synthesis of Bromo (Di-)Functional Polymers. Activators regenerated by electron transfer atom transfer radical polymerization (ARGET ATRP) protocols were adapted from the literature.[35] In a typical procedure, copper(I) bromide (13.6 mg, 0.09 mmol), tris[2-(dimethylamino)ethyl]amine (0.095 mmol, 278 µL, 0.34 mmol mL^{-1} in ansiole) and isobornyl acrylate (20 mL, 94.7 mmol) were dissolved in anisole (5 mL) in a flame dried Schlenk flask and degassed *via* nitrogen purging for 45 minutes. In two additional Schlenk flasks, butylene bis(2-bromoisobutyrate) (183.7 mg, 0.95 mmol) and tin(II) 2-ethylhexanoate (153 µL, 0.47 mmol) were dissolved in anisole (7.5 mL each) and degassed. Subsequently, the solutions were transferred into the first Schlenk flask *via* a cannula and stirred at 60 °C for 35 minutes. The polymerization was stopped in an ice bath and quenched with air at low conversion values (~25 %) in order to control for unwanted chain termination before filtration over neutral aluminum oxide and precipitation in cold methanol. The white polymer powder was dried *in vacuo* and characterized *via* SEC and ^{1}H NMR, evidencing a high bromo end group fidelity of consistently between 98-99 % for each synthesised polymer system *via* the comparison of initiator to end group signals (see **Table 1** for the full list of synthesized polymers, the ESI for the characterization data in **Figure S1-8** and the synthetic details of bromo monofunctional poly(methacrylates) in **Table S1** as well as the ones of bromo difunctional polyacrylates in **Table S2**†).

Synthesis of Cp (Di-)Functional Polymers. The synthetic procedure was adapted from the literature.[36] In a typical procedure, bromo difunctional poly(isobornyl acrylate) (3.0 g,

0.30 mmol), sodium iodide (545 mg, 3.63 mmol) and triphenyl phosphine (318 mg, 1.21 mmol) were dissolved in anhydrous THF (6.0 mL). Nickelocene (229 mg, 1.21 mmol) was added and the reaction mixture was stirred under argon at ambient temperature for 5 hours. The reaction was subsequently purged with air, filtered over basic aluminum oxide and the polymer was repeatedly precipitated in cold methanol. The off-white polymer was characterized *via* SEC and ^{1}H NMR to ensure quantitative conversion (see **Table 1** for the full list of synthesized polymers, the ESI for the characterization data in **Figure S1-8** and the synthetic details of the other Cp functionalized polymers in **Table S3**†).

Table 1 List of the synthesized bromo and Cp (di-)functional polymers, their number average molecular weight M_n, dispersity *Đ* and average number of repeating units *n*.

Polymer	M_n [g mol^{-1}]	*Đ*	*n*
BrPMMA	5600	1.19	52
BrP^{i}BuMA	7200	1.23	48
BrP^{t}BuMA	6800	1.19	45
Br$_2$P^{n}BuA	6600	1.07	49
Br$_2$P^{i}BuA	6800	1.07	50
Br$_2$P^{t}BuA	6600	1.08	49
Br$_2$PMA$_{large}$	4600	1.07	49
Br$_2$P^{i}BoA$_{large}$	9800	1.09	45
Br$_2$PMA$_{small}$	1200	1.04	9
Br$_2$P^{i}BoA$_{small}$	2300	1.05	9
CpPMMA	5600	1.16	52
CpP^{i}BuMA	7600	1.21	51
CpP^{t}BuMA	7200	1.16	48
Cp$_2$P^{n}BuA	6700	1.08	49
Cp$_2$P^{i}BuA	7000	1.07	52
Cp$_2$P^{t}BuA	6700	1.08	49
Cp$_2$PMA$_{large}$	4800	1.09	52
Cp$_2$P^{i}BoA$_{large}$	10200	1.12	47
Cp$_2$PMA$_{small}$	1300	1.06	11
Cp$_2$P^{i}BoA$_{small}$	2900	1.13	12

Synthesis of Diels–Alder Polymers/Adducts. In a typical procedure, cyclopentadiene difunctional poly(isobornyl acrylate) (50.0 mg, 0.005 mmol) and close to equimolar amounts of CDTE dilinker (around 4.0 mg, 0.005 mmol) were dissolved in anisole (200 µL) and heated to 120 °C for 10 minutes. The reaction was then slowly cooled to ambient temperature within 1 hour to achieve the DA step growth polymer with the desired amount of repeating units. The product was characterized *via* SEC, temperature dependent SEC and temperature dependent ^{1}H NMR (see ESI for the characterization data in **Figure S1-8** and the synthetic details for all DA polymers in **Table S4**†).

Characterization Techniques. Offline SEC was carried out on a Polymer Laboratories/Varian PL-GPC 50 Plus system, comprising an autosampler, a Polymer Laboratories 5.0 µm bead-size guard column (50 x 7.5 mm²), followed by three PL columns and a differential refractive index detector. Measurements were performed in THF at 35 °C with a flow rate of 1 ml·min^{-1}. The SEC system was calibrated using linear poly(methyl methacrylate) standards ranging from 800 g·mol^{-1} to 1.6·10^6 g·mol^{-1}. For analysis, appropriate Mark-Houwink-

Kuhn-Sakurada parameters were employed (**Table S5**†) and their integrity was assured *via* the comparison of initiator *vs.* an isolated backbone ^{1}H NMR signal for each respective polymer.[37-43]

^{1}H NMR spectra were measured on a Bruker Avance III 400 spectrometer with a CryoProbe at 400 MHz in CDCl$_3$ with 1024 scans for standard measurements and toluene-d$_8$ in a pressure tube for measurements at elevated temperatures. A sample concentration of 26.7 mg mL^{-1} was employed. Each DA polymer sample underwent the HT NMR measurements at all the desired temperatures from lower to higher ones, consecutively. After the stabilization of an adjusted temperature, the establishment of the equilibrium was ensured by repeated additional measurements with 16 scans before and after the actual measurement with 128 scans until no difference could be determined in the measured data anymore. The recyclability of the samples was checked after evaporation of the solvent and re-solvation. To compensate the varying shift of the signals at different measurement temperatures, the signals were adjusted to a polymer backbone signal. A baseline correction was conducted. The integration limits for the functional group signals were determined *via* the comparison with Cp functionalized polymers and DA adducts (**Figure S9**†).[14,21] The temperature dependent ratio of free Cp chain end groups to DA adducts and thus the degree of debonding (%$_{debond}$) was calculated as depicted in **Figure 1**.
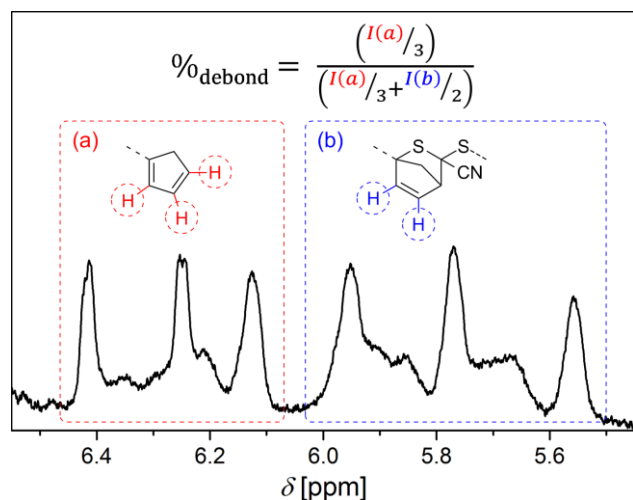

Figure 1 Calculation of the temperature dependent degree of debonding %debond via the 1H NMR signal ratios of (a) free Cp chain end groups and (b) closed HDA adducts.

A typical measurement and data processing error of on average ±2 % was determined *via* the two fold measurement of DA material from the same batch at different days.

Temperature dependent SEC was performed on a PL-GPC 220 high temperature chromatograph (Agilent Technologies), featuring a temperature controlled autosampler, column oven and dRI as well as viscosity detection. Separation was achieved through one PL ResiPore column (3 µm bead-size) and a mixture of 60 % 1,2,4-Tricholorobenzene (TCB) in *N,N*-Dimethylformamide (DMF) was employed as a solvent at a flow rate of 1 mL min^{-1}. Details regarding the evaluation of the chromatograms can be found in the Electronic Supplementary Information†.

Small-angle neutron scattering (SANS) measurements were carried out at the instrument D11 of the ILL in Grenoble with a wavelength of 6 Å and at two sample-detector distances of 8 m and 1.2 m, covering a broad q-range from 0.0083-0.0824 Å^{-1} (at 8 m) and 0.06-0.514 Å^{-1} (at 1.2 m) with a good overlap of the two q-regimes. The samples were measured at concentrations of approximately 1, 2, 3, 4 and 5 wt%. The solvent toluene-d$_8$ was also measured, normalized and then subtracted from the solution data. Data analysis was performed according to the procedure proposed by Casassa and Holtzer (see ESI for further information†).[44,45]

Computational Methods. Standard *ab initio* and density functional theory calculations were performed using Gaussian 09 software package.[46] The modeling was performed for a Diels–Alder reaction between the CDTE dilinker and Cp difunctional macromonomers with varying numbers of MA, ^{t}BuA, ^{i}BuA and ^{i}BoA building blocks. Calculations were based on the lowest energy isomers and conformers of the reactants and products (shown in **Scheme 2**), as identified by a screening carried out for the shortest difunctional macromonomers (*n = m = 0* and *n = m = 1*). The conformational searches in the gas phase were performed using an Energy-Directed Tree Search algorithm at the M06-2X/6-31G(d) level of theory.[47,48] For the longer species (*n = m = 2*) the starting geometries were constructed by incorporating the next monomer unit in the lowest energy conformer of *n = m = 1* and performing conformational searching only at the reaction center. For all gas-phase conformers within the lowest 10 kJ mol^{-1}, their geometries were subsequently relaxed and energies re-calculated in the presence of a solvent field (toluene), modeled using the SMD/M06-2X/6-31G(d) method. In this way the lowest-energy solution-phase conformers were obtained. Additionally, the extended chain conformers were obtained by fully unfolding the chains while keeping the conformation of the reaction center intact. Geometries of all these species were then refined at the M06-2X/6-31G(d) level of theory. Accurate energies were calculated using two-layer ONIOM-like approximation.
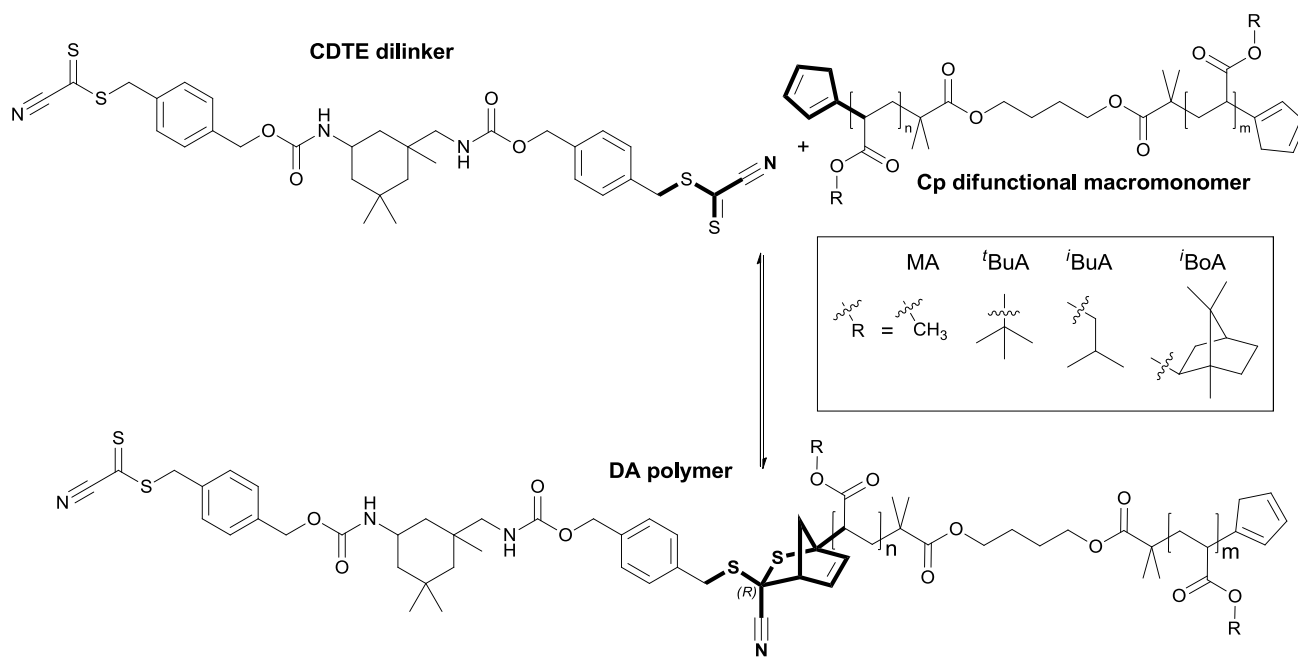
Scheme 2 Model DA reaction studied using quantum chemistry. Fragments in bold correspond to the core layer (reaction centre) in the ONIOM-like approximation.

The electronic energy of the reaction at the core layer was calculated using high-level composite *ab initio* G3(MP2)-RAD method, while M06-2X/6-31G(d) method was applied to the full system.[49] Gas-phase entropic and thermal corrections were evaluated from the M06-2X/6-31G(d) frequencies, scaled by the recommended scaling factors.[50] The Gibbs free energies of solvation in toluene were calculated using the SMD/M06-2X/6-31G(d) method.[51]

Results and Discussion

Theoretical Studies

To understand the entropic contributions to debonding, we conducted a quantum chemical study of oligomeric models of acrylate DA polymers. The selection of the polymers was carried out according to the steric properties of their side chain substituents, as discussed in the experimental studies section. The enthalpic and entropic contributions to the reaction Gibbs free energy were calculated for the Diels−Alder reactions between the CDTE dilinker and Cp difunctional macromonomers of MA, ^{t}BuA, ^{i}BuA and ^{i}BoA with chain lengths up to $n = m = 2$ (**Scheme 2**).

As in our previous study, we treated these species as being in the solution phase and analysed the entropic contributions to bonding in terms of the gas-phase vibrational, translational and rotational entropy and the remaining solvation energy contributions.[32] This treatment, accurate for small molecules in solution, over-simplifies the complexities of polymer – polymer reactions but has previously been shown to be qualitatively useful in understanding the characteristic chemical trends.[32] In

carrying out the calculations, we considered the reactants and products in their minimum energy conformations and also in modified conformations, where the conformation of the reaction centre itself was still fully optimized but the remaining polymer chains were extended into (optimized) linear conformations (**Figure 2**). The extended chain structures were considered because the minimum energy conformers, while providing the best representation of the oligomeric species studied computationally, are unlikely to be realistic representations of the longer chain polymeric species, where steric hindrance would prevent such globular structures from forming.
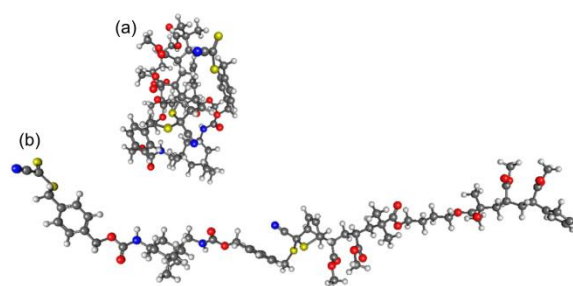

Figure 2 Optimized geometries of the DA adducts of CDTE and Cp$_2$PMA (with $n = m = 2$) corresponding to (a) the lowest energy conformation and (b) the extended chain conformation.

The calculated reaction entropy contributions for the various Diels−Alder reactions for both sets of conformers as a function of chain length are provided in **Figure 3**, while the overall predicted %$_{debond}$ *vs.* temperature graphs are provided in **Figure 4**.
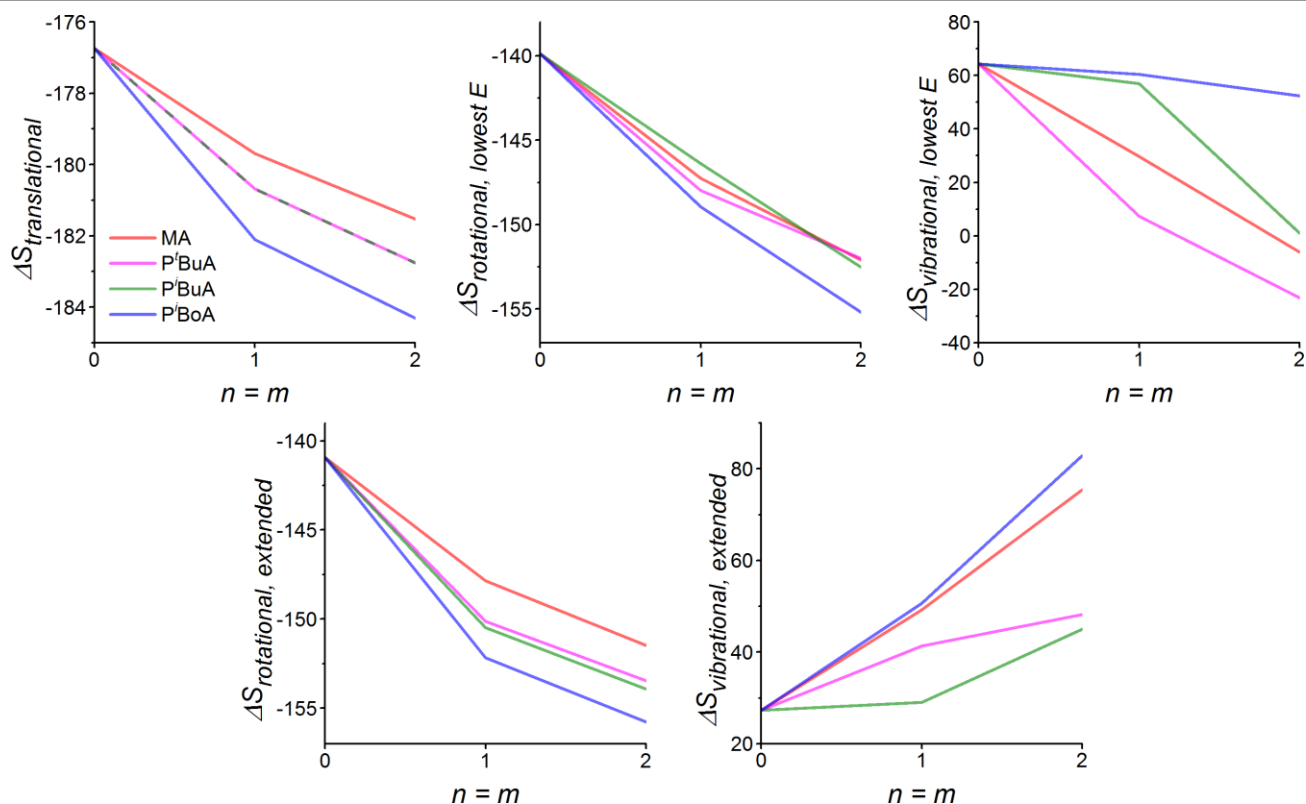
Figure 3 Calculated changes in the entropy (ΔS in J mol^{-1} K^{-1}) of model DA reactions for different *n, m* (chain lengths) of various acrylate macromonomers in their lowest energy or extended chain conformation. In these figures, the more negative ΔS, the lower the Gibbs free energy of bonding, or the greater the extent of debonding, at a given temperature.

Considering first **Figure 3**, we note that the translational entropy, being only dependent on mass, is independent of the conformer studied. Consistent with our previous study, ΔS_{trans} becomes more negative (and hence bonding becomes less favored and debonding temperatures are lowered accordingly) as the side chain mass is increased (MA < ^{t}BuA, ^{i}BuA < ^{i}BoA) and as the chain length of the linkers is increased.[32] The rotational entropy is dependent on both the total mass and its distribution (i.e. geometry) of the reaction participants, and hence, while a systematic trend is obtained for the linear (extended chain) conformers, results for lowest energy conformers are less coherent. For the extended conformers, the trends reinforce those for the translational entropy (*i.e.* MA < ^{t}BuA, ^{i}BuA < ^{i}BoA), with the heavier side chains contributing to lower debonding temperatures. For both sets of conformers, the chain length effects on ΔS_{rot} also reinforce those on ΔS_{trans}, with increasing chain length leading to lower debonding temperatures, again consistent with our earlier study.[32] Interestingly, the vibrational entropy contribution, which corresponds most closely to the phenomenological concept of 'chain stiffness', does not appear to follow any clearly determined trends and is qualitatively different between the two conformer scenarios, as well as between the different side chain substituents. Such a complicated picture is caused by the interplay between the number and intensities of vibrational modes, corresponding to both the newly forming bonds in the DA reactions and to the intramolecular bonding modes (e.g. H-bonds), and is thus highly dependent on the conformations of the reaction participants. However, one striking observation is that for both scenarios – but especially the lowest energy conformations – ^{i}BoA has the highest ΔS_{vib}. This counters to some extent the effect of its higher mass and bulk on ΔS_{trans} and ΔS_{rot}, both of which contribute to a greater extent of debonding compared with the other side chains. When the different entropic contributors, along with the bonding enthalpy and solvation energy, are combined to predict the effective %$_{debond}$ as a function of temperature (**Figure 4**), the trends are again dependent on the conformations used.
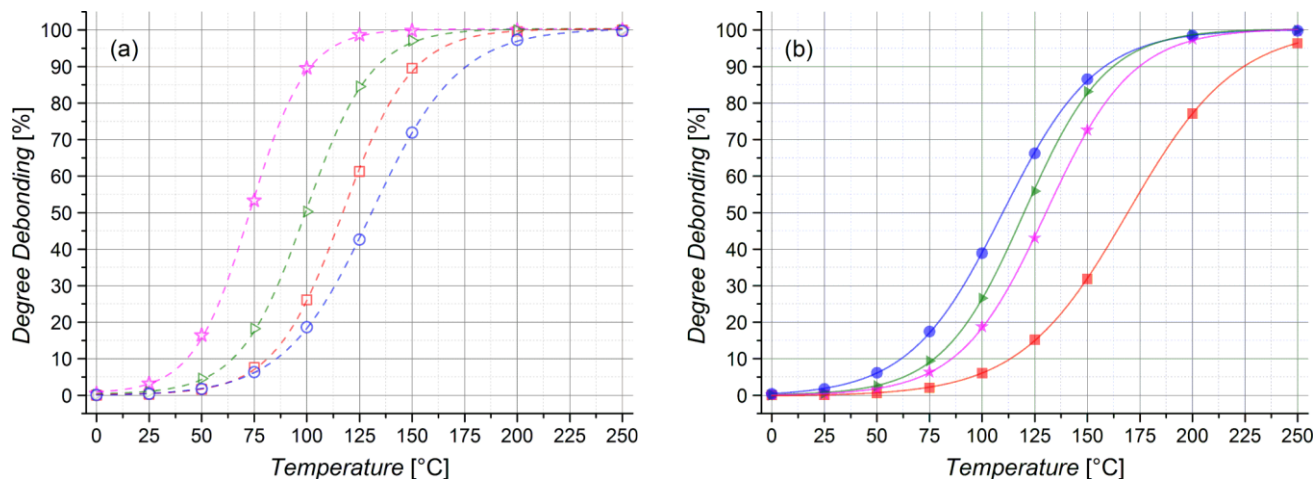
Figure 4 Degree of debonding (determined from the calculated reaction energies for $n = m = 2$ chain lengths) *vs.* temperature for (a) lowest energy and (b) extended chain conformers of P^{t}BuA (★), P^{i}BuA (▶), PMA (■) or P^{i}BoA (●).

In the case of the lowest energy conformations the bulkiest side chain substituent (^{i}BoA) is characterized with the highest debonding temperature. In contrast, for the extended chains, the debonding temperature decreases systematically with the bulk and mass of the side chain substituent, with ^{i}BoA now having the lowest debonding temperature. As we will show below, this dramatic trend reversal is mirrored in the differing experimental results for short (10 monomer units) and longer (50 monomer units) chains. Whilst the chains studied computationally are exceptionally short ($n = m = 2$ units) it would appear that the lowest energy (globular) conformers provide a reasonable model for the behavior of the shorter chains, while the extended conformers provide more realistic models for the longer ones. More generally, these calculations suggest that – in addition to the mass and chain length effects demonstrated previously[32] – polymer stiffness is likely to shape the polymer debonding behavior.

Experimental Studies

The realization of building blocks with well-defined lengths and masses that are connected *via* DA chemistry for the examination of entropic chain mass and length effects on the ligation chemistry can be achieved *via* the application of living controlled polymerization methods or the attachment of different substituents to a core molecule.[32] To also enable a choice of differently stiff polymer backbones, diverse methods were considered. As parameters such as persistence lengths, characteristic ratios or Mark-Houwink-Kuhn-Sakurada parameters are highly dependent on the given conditions and challenging in their determination – especially for short polymer chains – a more qualitative but universal approach was employed for a first selection of polymers.[52-55] The steric hindrance of the side chains of polymers, along with the backbone composition and electrostatic interactions, correlate with the polymer stiffness, as the polymer flexibility depends on the energy barriers between the different conformational states.[56] An alternative polymer characteristic, highly depending on the chain mobility and thus length and steric demand of the side chains, is the glass transition temperature T_g. Larger side chain end group volumes lead to decreasing chain mobility and thus higher T_g values, whereas an increase in free side chain length leads to facilitated chain movement and thereby to lower T_g values due to internal plasticizing effects.[34,57] Of course, T_g values are characteristics for polymer melts and cannot be transferred directly to behavior in solution where interactions between polymer and solvent are essential.[58] In addition, the chain length dependency of T_g is neglected, as only the relative differences of chains with the same amount of repeating units are of interest in the current study.[59] However, if equal polymer backbones of equal length with different homonuclear side chain substituents are investigated, their T_g values should correlate approximately with chain stiffness. Therefore, diverse polyacrylates and, in addition, some poly(methacrylates) with significantly differing T_g values were considered in the current study, as collated in **Table 2**.

Table 2 The different poly(meth-)acrylates investigated in the current study and the corresponding literature values for their glass transition temperatures T_g as well as measured persistence lengths (l_p) for the poly(butyl acrylates).

| Polymer	T_g [°C]	Ref.	l_p [nm]
poly(methyl methacrylate)	105	60,61	
poly(iso-butyl methacrylate)	48	62	
poly(tert-butyl methacrylate)	118	63,64	
poly(n-butyl acrylate)	-54	61	2.0
poly(iso-butyl acrylate)	-24	65	1.8
poly(tert-butyl acrylate)	43	66	2.3
poly(methyl acrylate)	8	61,66	
poly(isobornyl acrylate)	95	66	

To confirm the assumption of a correlation between T_g and polymer stiffness and to include solvent effects, the persistence lengths (l_p) of the three important isomeric poly(butyl acrylates) were determined *via* SANS measurements in the solvent that was applied for the HT NMR experiments and in the computational calculations. It can be seen in **Table 2** that the solvent effects

should not be underestimated, as poly(*n*-butyl acrylate) has a higher persistence length than its *iso*-butyl derivative. Still, a sufficiently large difference between the T_g values of comparable polymers can serve as a guide for their relative chain stiffness.

The diversely substituted poly(meth-)acrylates were chosen to afford polymeric building blocks varying in stiffness and mass, which can be linked to form (A,A'-) diblock or DA step growth polymers *via* DA chemistry. The resulting library of polymeric materials was used to study the previously reported chain mass and length effect as well as the proposed chain stiffness effect. As increasing chain mass and length could be shown to lead to substantially decreased debonding temperatures of DA adducts due to the higher amounts of released entropy during the scission of heavier and longer building blocks, different isomeric butyl (meth-)acrylates were also included in the selection to control for the entropic chain mass effect and allow an isolated investigation of a hypothetical chain stiffness effect.[32,34]

Three experimental approaches were adopted to investigate the different types of entropic effects on the ligation chemistry: (i) (A,A'-) block copolymers based on building blocks of the same length, yet differing in mass or stiffness, (ii) DA polymers with building blocks of the same length, but differing in mass or stiffness and (iii) DA polymers with basic units of different chain lengths, masses and stiffness with subsequent temperature dependent characterization of their DA equilibrium (**Scheme 1**). Below, the three approaches and the obtained results are discussed systematically.

(A,A'-) Diblock approach with equal building block sizes. As discussed in the Introduction, we will first investigate diblock polymers of identical chain length. To compare the temperature dependent degree of debonding of polymer chains, which are linked *via* DA chemistry and are bearing different side chain groups – which also means that the respective chains have different T_g and chain mobilities – Cp end group monofunctional poly(methyl methacrylate) (PMMA), poly(*iso*-butyl methacrylate) (P*i*BuMA) and poly(*tert*-butyl methacrylate) (P*t*BuMA) building blocks with approximately 50 repeating units were synthesized. To enable the DA linkage reaction, the Cp protected CDTE dilinker was deprotected at 120 °C (**Scheme 3**).
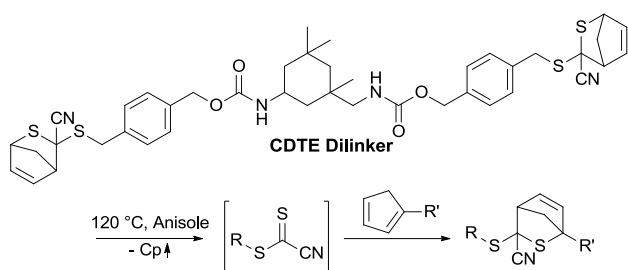
Scheme 3 HDA linkage of Cp functional polymers *via* a CDTE dilinker.

The dissolution of all reaction compounds in anisole enables the evaporation of the released Cp and a dynamic protection of the exposed CDTE group with the Cp polymer end groups to prevent unwanted side reactions. During the following cooling phase, the

actual HDA reaction takes place. While not being stereoselective, the more important feature for our application is its catalyst-free character. The three poly(methacrylate) blocks were each coupled to afford diblock polymers in a HDA reaction *via* the CDTE dilinker (see **Figure 5** for an exemplary SEC data set, **Figure S1** for the molecular size dependent chromatograms and thus the size distributions of the other employed polymers measured *via* offline SEC†).
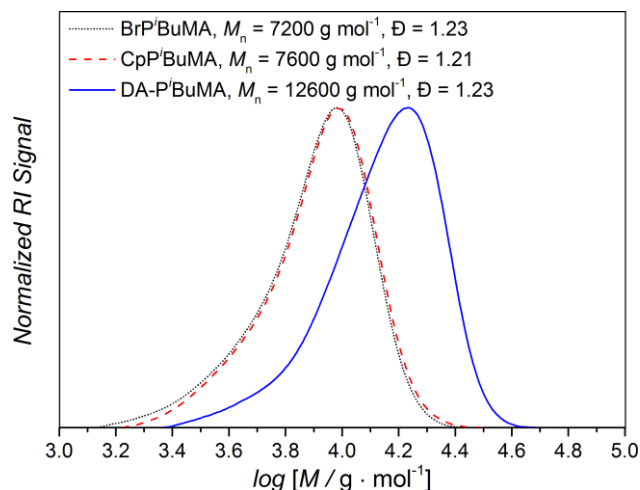

Figure 5 Exemplary SEC chromatograms of the bromo precursor polymer (····), Cp functional building block (----) and Diels–Alder diblock polymer (——) for 50 *iso*-butyl methacrylate repeating units per building block (see **Figure S1** for the chromatograms of the other employed polymers†).

Even though there will always be a small population of unreactive species due to irreversible chain termination events during the synthesis of the utilized building blocks, the careful implementation of a living controlled polymerization technique and the quantitative subsequent functionalization in combination with a thorough characterization as well as the readily proceeding ligation chemistry allows for the conclusion that only an insignificant concentration of non-functional reactants is present. Thus, no substantial effect on the investigated reaction equilibria while guaranteeing the comparability of different samples is given. The application of monofunctional methacrylates should enable experiments without unwanted Cp-Cp self-dimerization due to their low chain mobility. Further, dimerized chains do not impair the measurements due to their lost functionality for further DA reactions and insignificant degree of debonding at the temperatures under investigation. In addition, the macromonomers can easily be precipitated and thus permit facile handling. As – in contrast to our previous study – the applied DA system enables very fast switching times between closed DA adducts and open chain ends, the resulting specimens could be characterized *via* high temperature (HT) ^{1}H NMR spectroscopy at temperatures ranging from 40 to 140 °C and the respective ratios of open Cp chain ends to HDA adduct signals were calculated as the temperature dependent degree of debonding (**Figure 1**), enabling a very facile, straightforward and fast analysis.[14,32] Comparing the results of the three methacrylate diblock polymers in **Figure 6**, a clear effect of the

different chain nature on the degree of debonding is observed, as the sample with P^{i}BuMA building blocks has the highest degree of debonding at any given temperature, followed by P^{t}BuMA and finally PMMA.
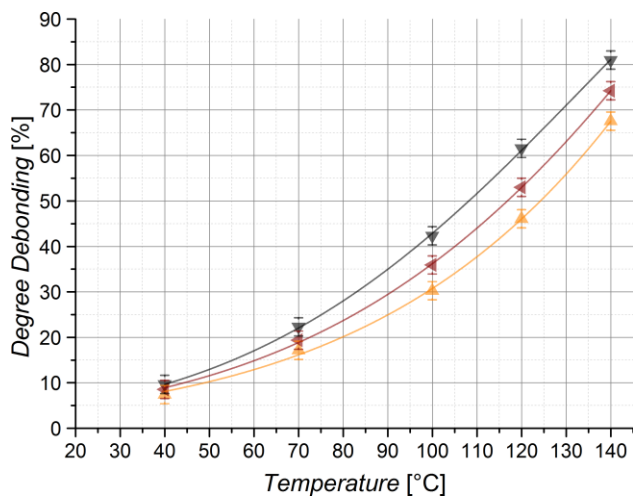

Figure 6 Temperature dependent degree of debonding for Diels–Alder A,A'-type diblockcopolymers consisting of PMMA (▲), P^{i}BuMA (▼) or P^{t}BuMA (◄) building blocks with a length of 50 repeating units assessed by HT NMR spectroscopy.

These experimental data as well as the range of the debonding values is reproduced by the quantum chemical calculations for the extended acrylate chain conformers with the same side chain substituents (**Figure 4 (b)**), enabling a clear assignment of the entropic causes. Considering the previously reported chain mass effect, it comes at no surprise that the two butyl methacrylate building blocks with heavier side chain groups enable a 7 – 14 % higher degree of debonding than the methyl methacrylate ones of the same chain length.[32] In contrast, the difference of 7 % in debonding of the two butyl methacrylate building blocks of the same chain length and thus the same chain weight must be underpinned by yet another effect. An explanation could be the difference in chain stiffness, as the degrees of vibrational and rotational freedom of the connected chains get reduced by chain scission. When polymer chains are divided into smaller pieces, flexibility and thus rotational and vibrational entropy is lost. With P^{i}BuMA having a lower T_g value than P^{t}BuMA – implying the P^{i}BuMA building blocks have a higher chain mobility than the P^{t}BuMA ones of the same length – P^{i}BuMA chains are less impaired by the entropic confinement and thus their debonding is less hindered (= more favored) than the one of P^{t}BuMA, leading to a chain stiffness effect. This is again reflected in the rotational and vibrational ΔS charts, theoretically calculated for the extended chains scenario for acrylates (**Figure 3**), in which these values for DA reaction are lower in the case of ^{i}BuA, corresponding to its lower debonding temperature. Remarkably, the stiffness effect is overcompensated by the mass effect when comparing PMMA and P^{t}BuMA samples, where the stiffer but also heavier P^{t}BuMA has the higher degree of debonding, allowing a first insight into the specificity of these two properties.

DA polymer approach with equal building block sizes. We next expanded our study to include DA step growth polymers of the CDTE dilinker and Cp difunctional acrylate macromonomers. Thus, a possible impact of the larger building block dispersity (ca. 1.2) and therefore the presence of a larger number of different chain lengths and masses on the results of the examined A,A'-type diblockcopolymer methacrylate systems (**Figure 6**) as well as the challenging diblock formation could be addressed. The low dispersity of the polyacrylate building blocks (close to 1.1 or less, **Table 1**) can be utilized to achieve more accurate results. In addition, the larger size change from building block to DA polymer facilitated the analysis *via* SEC techniques. Furthermore, the use of DA step-growth polymers with multiple ligation sites in one molecule should lead to an enhancement of the examined effects due to the higher amount of entropy released during chain scission reactions. To achieve comparable results in the following measurements, an average degree of polymerization (DP_n) of 6 was targeted for these DA polymers under similar reaction conditions (**Scheme 3**) to those for the DA block copolymer formation (see **Figure 7** for an exemplary SEC data set, **Figure S2** for the chromatograms of the other employed polymers, **Equation S1** for the calculation of the DP_n†). A control sample of every macromonomer without dilinker was exposed to the same reaction conditions to ensure that the desired HDA reaction and not the unwanted Cp-Cp dimerization had occurred.
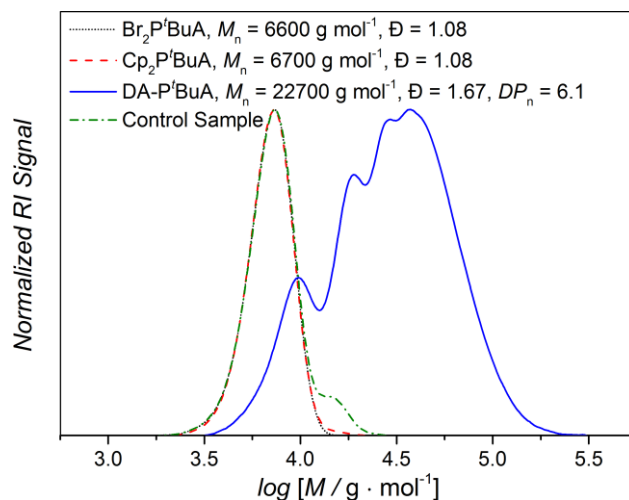

Figure 7 Exemplary SEC chromatograms of the dibromo precursor polymer (⋯⋯), Cp difunctional macromonomer (- - - -), Diels–Alder polymer (——) and control sample of heated Cp difunctional macromonomer without CDTE dilinker (-·-·-) for 50 *tert*-butyl acrylate repeating units (see **Figure S2** for the chromatograms of the other employed polymers†).

To allow a mass effect free analysis, isomeric poly(*n*-butyl acrylate) (P^{n}BuA), poly(*iso*-butyl acrylate) (P^{i}BuA) and poly(*tert*-butyl acrylate) (P^{t}BuA) macromonomers of the same chain length (50 repeating units) were also studied. From HT ^{1}H NMR characterization at temperatures ranging from 25 to 140 °C, it is evident that the stiffest polymer, P^{t}BuA, displays the expected lowest degree of debonding at a given temperature (**Figure 8**) and the experimental results for P^{t}BuA and P^{i}BuA are

again in good agreement with the quantum chemical calculations for extended chain conformers (**Figure 4 (b)**).
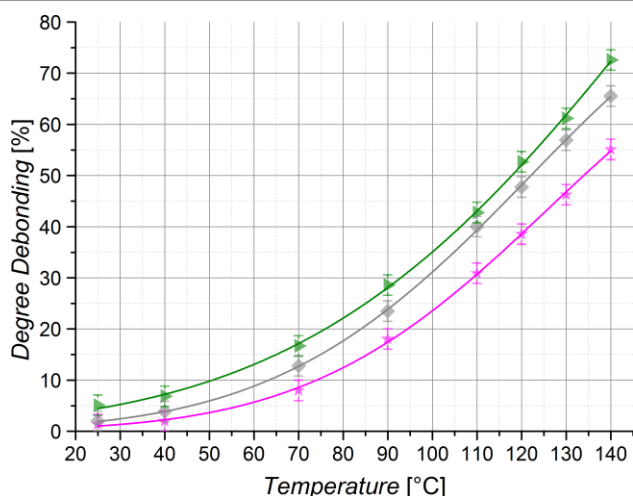

Figure 8 Temperature dependent degree of debonding for Diels–Alder polymers consisting of Cp difunctional P^{i}BuA (▶), P^{n}BuA (◆) or P^{t}BuA (★) building blocks with a length of 50 repeating units and CDTE dilinker assessed by HT NMR spectroscopy.

Although P^{n}BuA has the lowest T_g of the three investigated poly(butyl acrylates), it has not the lowest persistence length (**Table 2**) and thus chain stiffness in the solvent employed for the HT NMR measurements (toluene-d_8). Indeed, Coelho *et al.* previously reported that in THF P^{i}BuA is the least stiff of these three polymers.[53] Moreover, the solvent is known to affect chain conformation and the model calculations presented above clearly show the effect of chain conformation on the debonding temperature (i.e., globular chains give rise to lower debonding temperatures compared to the corresponding extended chain conformation, refer to **Figure 2** and **Figure 4**). The order of the

stiffness values of the examined chains and thus the hypothetically linked degrees of debonding are a consequence of solvent effects – as a result, the debonding values of P^{n}BuA at 140 °C lie 11 % above the ones of P^{t}BuA, yet 7 % below the ones of P^{i}BuA. Accordingly, the degree of debonding of the investigated DA polymers could be adjusted in a range of nearly 20 % by merely changing the structure of the building block side chains without changing their length or mass, clearly evidencing the existence of an effect of the polymer side chain groups on the bonding reaction properties.

In order to investigate the debonding behavior in more detail, the rDA reaction of the DA polymers was also investigated using temperature dependent size exclusion chromatography (TD SEC). Monitoring the molar mass distribution of the polymers during the rDA reactions provides further insights into the process of the debonding reactions. **Figure 9 (a)** shows chromatograms of DA-P^{t}BuA at 80 °C at different reaction times. With increasing reaction time, the peak shifts towards lower molar masses (higher elution volume) and the width of the peak decreases and eventually converges to the shape of the building block. In **Figure 9 (b)** only one chromatogram is shown with the calculated individual peaks of the DA polymer, the respective building block and the CDTE dilinker molecule. Simple calculations of molar mass averages with respect to polymer standards are not possible from these chromatograms, and a different approach for their evaluation has been chosen, in which the concentration decrease of the DA polymer is being tracked during the rDA reaction. The obtained values reflect the excess of the rDA reaction but cannot be compared directly to the degree of debonding obtained by NMR as the part of the rDA reaction that only releases small linker molecules is not captured by the calculations due to the small weight and thus elution time differences as well as overlapping signals (for detailed information on the SEC analysis see the ESI†).
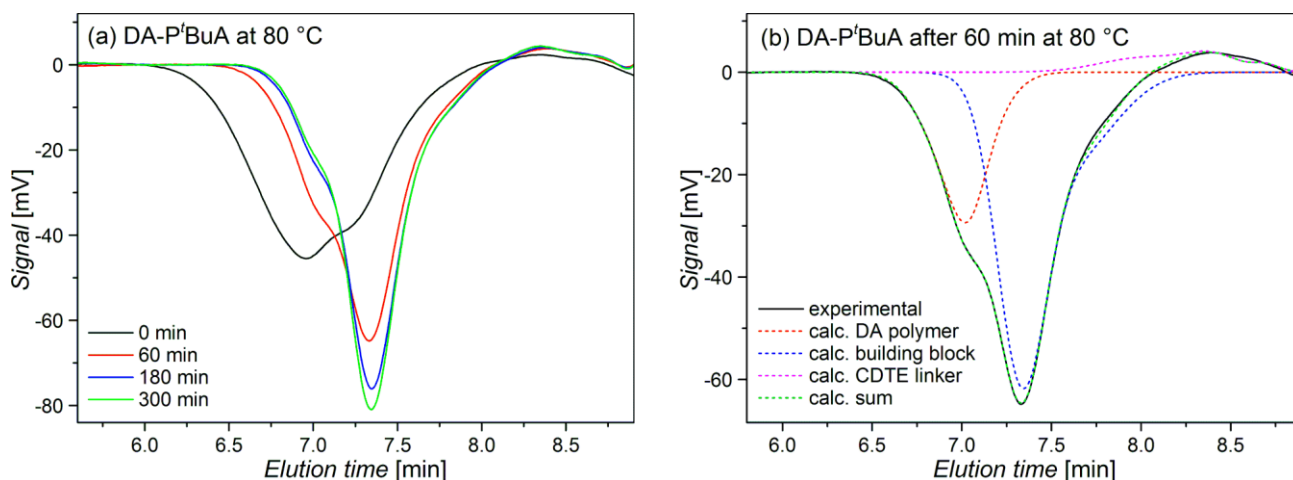

Figure 9 TD SEC chromatograms, (a) DA-P^{t}BuA after different rDA times at 80 °C in 60 % TCB and 40 % DMF, (b) DA-P^{t}BuA after 60 min. rDA at 80 °C and distributions calculated by peak deconvolution of the individual components.
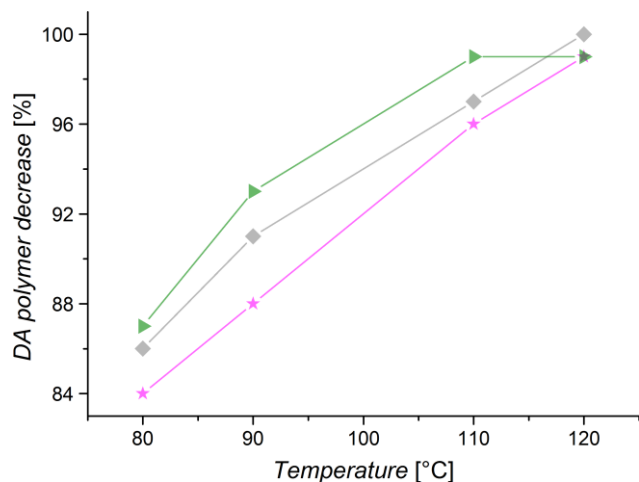
Figure 10 TD SEC results: decrease of concentration of DA polymers due to rDA reactions of the DA polymers consisting of Cp difunctional P^{i}BuA (▶), P^{n}BuA (◆) or P^{t}BuA (★) building blocks with a length of 50 repeating units and CDTE dilinker.

Figure 11 Temperature dependent degree of debonding for Diels–Alder polymers consisting of Cp difunctional PMA$_{large}$ (■, 50 repeating units), P^{i}BoA$_{large}$ (●, 50 repeating units), PMA$_{small}$ (□, 10 repeating units) or P^{i}BoA$_{small}$ (○, 10 repeating units) building blocks and CDTE dilinker assessed by HT NMR spectroscopy.

Figure 10 shows the obtained DA-Polymer concentration decreases for P^{i}BuA, P^{n}BuA, and P^{t}BuA. The graph shows that P^{n}BuA exhibits the most pronounced decrease of DA polymer, followed by P^{i}BuA and P^{t}BuA, and, thus, reproduces the trend of the T_g values observed for the three polymers. As already noted, the stiffness of polymers in solution is affected by the thermodynamic properties of the solvent and consequently the order may vary depending on the solvent. This could be a possible reason for the deviation in the debonding behavior of P^{i}BuA and P^{n}BuA analyzed in different solvents by TD SEC and HT NMR. Nevertheless, the significance of different side chain substituents and their impact on the ligation chemistry is again clearly illustrated, additionally emphasizing the importance of the applied solvent.

DA polymer approach with differing building block sizes. To finally compare the mass and chain stiffness effects and their impact at different chain lengths, a further set of samples was prepared. Diels–Alder macromonomers with very different side chain groups, namely Cp difunctional poly(methyl acrylate) (PMA) and poly(isobornyl acrylate) (P^{i}BoA), were synthesized with two chain lengths each and underwent the described DA step growth polymerization with the CDTE dilinker (see **Figure S3+4** for the SEC chromatograms of the employed polymers†). It is expected that the stiffness effect on the chain scission of longer building blocks is less pronounced than the one of smaller building blocks, as longer chain sections still have more degrees of freedom and thus their liberation should be less hindered. Inspection of the debonding values of the DA polymers synthesized from reasonably long macromonomers with 50 repeating units (**Figure 11**) indicates that the heavier macromonomer P^{i}BoA$_{large}$ has more than 10 % higher debonding values than PMA$_{large}$, leading to the conclusion that for long chains the chain stiffness effect becomes less important and is surpassed by the mass effect.
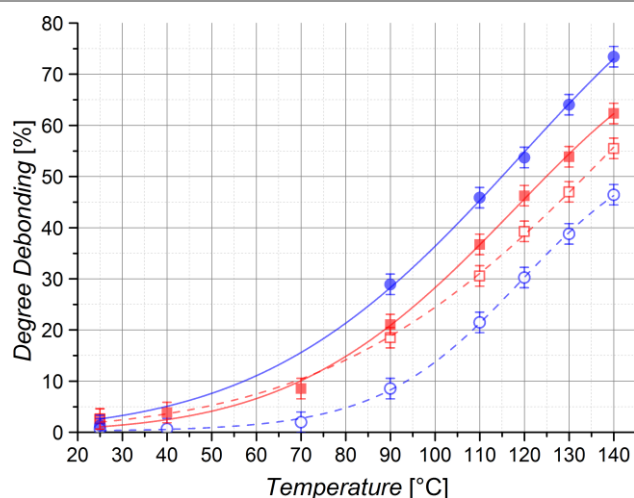
To decrease the freely jointed chain character of the building blocks by decreasing their contour length, DA polymers based on macromonomers with 10 acrylate repeating units (PMA$_{small}$ and P^{i}BoA$_{small}$) were examined.[67] The previously described chain length and mass effect is reproduced, as the observed debonding values decrease for shorter and thus also lighter chains of the same polymer type when comparing the debonding values for PMA$_{small/large}$ as well as P^{i}BoA$_{small/large}$ (**Figure 11**). Interestingly, the values for PMA$_{small}$ and P^{i}BoA$_{small}$ macromonomers indicate that the chain mass effect is now overcompensated by the stiffness effect, as the debonding values for the lighter PMA$_{small}$ even surpasses the ones of the heavier P^{i}BoA$_{small}$ sample by nearly 10 %, clearly confirming the assumption of a growing influence of the stiffness effect with decreasing chain length due to the more impaired chain mobility of the separated building blocks. Indeed, as foreshadowed above, these trends for shorter chains are in qualitative agreement with the quantum chemical trends for the calculations performed on (globular) lowest energy conformations, where such mobility is expected to be hampered (**Figure 4 (b)**). In contrast, the experimental trends for the longer chains qualitatively follow the quantum chemical trends based on extended chains (**Figure 4 (a)**). In other words, shorter chains are able to coil better, whereas longer chains stay largely extended.

Investigating the same set of DA polymers by TD SEC was not possible as in the case of PMA$_{small}$ and P^{i}BoA$_{small}$ the peaks of the DA polymer, the building block and the CDTE dilinker overlap too strongly for a precise analysis. PMA$_{large}$ and P^{i}BoA$_{large}$ however could be analysed very precisely and can reproduce very well the trend that the stiffness effect is overcompensated by the mass effect and – as a consequence – the rDA reaction proceeds further for P^{i}BoA than for PMA (**Figure 12**).
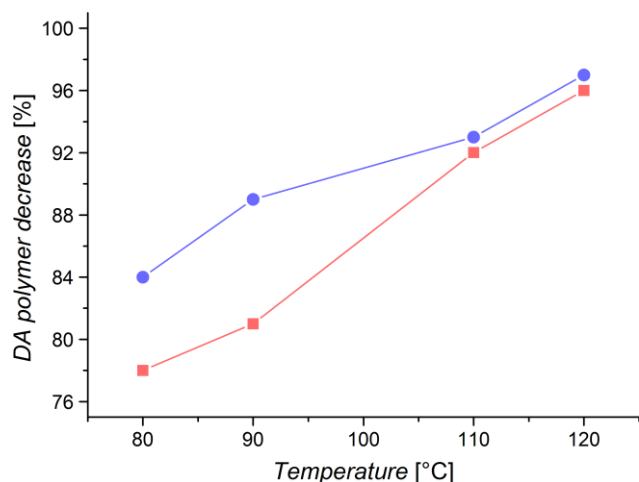
Chemical Science Accepted Manuscript

Figure 12 TD SEC results: decrease of concentration of DA polymer due to rDA reaction of the DA polymers consisting of Cp difunctional PMA_{large} (■, 50 repeating units) and P^iBoA_{large} (●, 50 repeating units) building blocks and CDTE dilinker.

Conclusions

Strong entropic chain effects on chain linking and scission reactions are observed for Diels–Alder step-growth and diblock polymers *via* HT NMR and TD SEC experiments. Not only could the previously published chain length and mass effect be excellently reproduced with other Diels–Alder polymer systems enabling the adjustment of the temperature dependent degree of debonding by approximately 30 % for the investigated P^iBoA macromonomers of different chain lengths, but also a large chain stiffness effect could be identified, which enables the modification of the reaction equilibrium between free and linked chains by up to approximately 20 % at 140 °C for different isomeric poly(butyl acrylate) chains of the same length and mass. Moreover, the impact of the chain stiffness effect was found to increase with decreasing chain length, as the chain mobility originates more and more from the local flexibility and less from the freely jointed character of a long polymer chain. While for the comparison of long chains, the heavier and stiffer P^iBoA system has higher debonding values than PMA – overcompensating any stiffness effect *via* the mass effect – for short chains the much lighter, but also less stiff PMA has significantly higher debonding values. In summary, it could be experimentally shown that not only higher molecular masses and longer chains, but also lower molecular stiffness values favor the debonding of ligated species, thus evidencing the manifold molecular characteristics that have to be considered when planning and executing reversible reactions. The experimentally observed trends can be reproduced and explained *via* quantum chemical calculations, leading to a better understanding of the fundamental principles of entropic effects on reversible bonding/debonding systems. The complex interplay of translational, rotational and vibrational entropy and their conformational dependencies are illustrated and it is shown that the better coiling ability accounts for the increased impact of chain stiffness of shorter and thus sterically less hindered chains on bonding reactions, in addition giving an explanation for

differing debonding values in solvents of different thermodynamic properties. The new insight into different chain effects in general and a chain stiffness effect in particular can be utilized to tune the processing and application temperatures of materials *via* the incorporation of different easily accessible backbones and their entropic effects without the need to change the underlying ligation chemistry. Our findings thus have the potential to invoke a step change in the design approach taken for self-healing or other smart materials, such as post-formable organic sheets *via* using physical rather than chemical parameters. Further – and importantly – the entropic chain length, mass and stiffness effects have to be kept in mind when ligation chemistry is transferred from small molecules to polymers or other large systems with significantly different entropic properties, as their impact on the molecule and material properties can be substantial.

Acknowledgements

Notes and References

[a] Preparative Macromolecular Chemistry, Institut für Technische Chemie und Polymerchemie, Karlsruhe Institute of Technology (KIT), Engesserstr. 18, 76131 Karlsruhe, Germany. E-mail: christopher.barner-kowollik@kit.edu

[b] Institut für Biologische Grenzflächen, Karlsruhe Institute of Technology (KIT), Hermann-von-Helmholtz-Platz 1, 76344 Eggenstein-Leopoldshafen, Germany.

[c] Leibniz-Institut für Polymerforschung Dresden, Hohe Strasse 6, 01069 Dresden, Germany. E-Mail: lederer@ipfdd.de

[d] Technische Universität Dresden, 01062 Dresden, Germany.

[e] ARC Centre of Excellence for Electromaterials Science, Research School of Chemistry, Australian National University, Canberra, ACT 0200, Australia. E-mail: michelle.coote@anu.edu.au

[f] Institut Laue-Langevin (ILL), 6 Rue Jules Horowitz, 38042 Grenoble, France.

[g] Evonik Industries AG, Paul-Baumann-Strasse 1, 45764 Marl, Germany.

† Electronic Supplementary Information (ESI) available: Synthetic details, applied MHKS parameters, SEC chromatograms of all samples, (HT) NMR data, experimental debonding values, SANS measurements, computational data (energy contributions and geometries in the form of Gaussian archive entries). See DOI: 10.1039/b000000x/

1. O. Diels and K. Alder, *Liebigs Ann. Chem.*, 1928, **460**, 98-122.

2. H. C. Kolb, M. G. Finn and K. B. Sharpless, *Angew. Chem. Int. Ed.*, 2001, **40**, 2004-2021.

3. N. K. Devaraj, R. Weissleder and S. A. Hilderbrand, *Bioconjugate Chem.*, 2008, **19**, 2297-2299.

4. S. Sinnwell, A. J. Inglis, T. P. Davis, M. H. Stenzel and C. Barner-Kowollik, *Chem. Commun.*, 2008, 2052-2054.

5. K. C. Nicolaou, S. A. Snyder, T. Montagnon and G. Vassilikogiannakis, *Angew. Chem. Int. Ed.*, 2002, **41**, 1668-1698.

6. H. Durmaz, B. Colakoglu, U. Tunca and G. Hizal, *J. Polym. Sci., Part A: Polym. Chem.*, 2006, **44**, 1667-1675.

7. M. Langer, J. Brandt, A. Lederer, A. S. Goldmann, F. H. Schacher and C. Barner-Kowollik, *Polym. Chem.*, 2014, **5**, 5330-5338.

8. J. R. McElhanon and D. R. Wheeler, *Org. Lett.*, 2001, **3**, 2681-2683.

9. A. A. Kavitha and N. K. Singha, *ACS Appl. Mater. Inter.*, 2009, **1**, 1427-1436.

10. A. J. Inglis, S. Sinnwell, M. H. Stenzel and C. Barner-Kowollik, *Angew. Chem. Int. Ed.*, 2009, **48**, 2411-2414.

11. M. A. Tasdelen, *Polym. Chem.*, 2011, **2**, 2133-2145.

12. A. S. Goldmann, T. Tischer, L. Barner, M. Bruns and C. Barner-Kowollik, *Biomacromolecules*, 2011, **12**, 1137-1145.

13. T. Pauloehrl, G. Delaittre, V. Winkler, A. Welle, M. Bruns, H. G. Boerner, A. M. Greiner, M. Bastmeyer and C. Barner-Kowollik, *Angew. Chem. Int. Ed.*, 2012, **51**, 1071-1074.

14. K. K. Oehlenschlaeger, N. K. Guimard, J. Brandt, J. O. Mueller, C. Y. Lin, S. Hilf, A. Lederer, M. L. Coote, F. G. Schmidt and C. Barner-Kowollik, *Polym. Chem.*, 2013, **4**, 4348-4355.

15. M. Glassner, K. K. Oehlenschlaeger, A. Welle, M. Bruns and C. Barner-Kowollik, *Chem. Commun.*, 2013, **49**, 633-635.

16. A. V. Samoshin, C. J. Hawker and J. Read de Alaniz, *ACS Macro Lett.*, 2014, 753-757.

17. X. Chen, M. A. Dam, K. Ono, A. Mal, H. Shen, S. R. Nutt, K. Sheran and F. Wudl, *Science*, 2002, **295**, 1698-1702.

18. E. B. Murphy, E. Bolanos, C. Schaffner-Hamann, F. Wudl, S. R. Nutt and M. L. Auad, *Macromolecules*, 2008, **41**, 5203-5209.

19. N. K. Guimard, K. K. Oehlenschlaeger, J. Zhou, S. Hilf, F. G. Schmidt and C. Barner-Kowollik, *Macromol. Chem. Phys.*, 2012, **213**, 131-143.

20. S. Billiet, X. K. D. Hillewaere, R. F. A. Teixeira and F. E. Du Prez, *Macromol. Rapid Commun.*, 2013, **34**, 290-309.

21. K. K. Oehlenschlaeger, J. O. Mueller, J. Brandt, S. Hilf, A. Lederer, M. Wilhelm, R. Graf, M. L. Coote, F. G. Schmidt and C. Barner-Kowollik, *Adv. Mater.*, 2014, **26**, 3561-3566.

22. S. Billiet, K. De Bruycker, F. Driessen, H. Goossens, V. Van Speybroeck, J. M. Winne and F. E. Du Prez, *Nat. Chem.*, 2014, **6**, 815-821.

23. S. D. Bergman and F. Wudl, *J. Mater. Chem.*, 2008, **18**, 41-62.

24. C. Dry, *Int. J. Mod. Phys. B*, 1992, **6**, 2763-2771.

25. S. R. White, N. R. Sottos, P. H. Geubelle, J. S. Moore, M. R. Kessler, S. R. Sriram, E. N. Brown and S. Viswanathan, *Nature*, 2001, **409**, 794-797.

26. J. P. Kennedy and K. F. Castner, *J. Polym. Sci. Pol. Chem.*, 1979, **17**, 2039-2054.

27. W. H. Binder, *Self-Healing Polymers*, Wiley-VCH, Weinheim, Germany, 2013.

28. J. Zhou, N. K. Guimard, A. J. Inglis, M. Namazian, C. Y. Lin, M. L. Coote, E. Spyrou, S. Hilf, F. G. Schmidt and C. Barner-Kowollik, *Polym. Chem.*, 2012, **3**, 628-639.

29. A. J. Inglis, L. Nebhani, O. Altintas, F. G. Schmidt and C. Barner-Kowollik, *Macromolecules*, 2010, **43**, 5515-5520.

30. M. Watanabe and N. Yoshie, *Polymer*, 2006, **47**, 4946-4952.

31. T. A. Plaisted and S. Nemat-Nasser, *Acta Mater.*, 2007, **55**, 5684-5696.

32. N. K. Guimard, J. Ho, J. Brandt, C. Y. Lin, M. Namazian, J. O. Mueller, K. K. Oehlenschlaeger, S. Hilf, A. Lederer, F. G. Schmidt, M. L. Coote and C. Barner-Kowollik, *Chem. Sci.*, 2013, **4**, 2752-2759.

33. J. Brandt, K. K. Oehlenschlaeger, F. G. Schmidt, C. Barner-Kowollik and A. Lederer, *Adv. Mater.*, 2014, **26**, 5758-5785.

34. C. Cao and Y. Lin, *J. Chem. Inf. Comp. Sci.*, 2003, **43**, 643-650.

35. W. Jakubowski and K. Matyjaszewski, *Angew. Chem. Int. Ed.*, 2006, **45**, 4482-4486.

36. A. J. Inglis, T. Paulöhrl and C. Barner-Kowollik, *Macromolecules*, 2009, **43**, 33-36.

37. D. A. P. R. A. Hutchinson, Jr, J. H. McMinn, S. Beuermann, R. E. Fuller, C. Jackson, *DECHEMA Monogr.*, 1995, **131**, 467–492.

38. B. Dervaux, T. Junkers, M. Schneider-Baumann, F. E. Du Prez and C. Barner-Kowollik, *J. Polym. Sci., Part A: Polym. Chem.*, 2009, **47**, 6641-6654.

39. H. L. Wagner, *J. Phys. Chem. Ref. Data*, 1985, **14**, 1101-1106.

40. G. E. Roberts, T. P. Davis, J. P. A. Heuts and G. E. Ball, *Macromolecules*, 2002, **35**, 9954-9963.

41. R. A. Hutchinson, S. Beuermann, D. A. Paquet and J. H. McMinn, *Macromolecules*, 1997, **30**, 3490-3493.

42. S. Beuermann, D. A. Paquet, J. H. McMinn and R. A. Hutchinson, *Macromolecules*, 1996, **29**, 4206-4215.

43. E. Penzel and N. Goetz, *Angew. Makromol. Chem.*, 1990, **178**, 191-200.

44. E. F. Casassa, *J. Chem. Phys.*, 1955, **23**, 596-597.

45. A. Holtzer, *J. Polym. Sci.*, 1955, **17**, 432-434.

46. G. W. T. M. J. Frisch, H. B. Schlegel, G. E. Scuseria, M. A. Robb, J. R. Cheeseman, G. Scalmani, V. Barone, B. Mennucci, G. A. Petersson, H. Nakatsuji, M. Caricato, X. Li, H. P. Hratchian, A. F. Izmaylov, J. Bloino, G. Zheng, J. L. Sonnenberg, M. Hada, M. Ehara, K. Toyota, R. Fukuda, J. Hasegawa, M. Ishida, T. Nakajima, Y. Honda, O. Kitao, H. Nakai, T. Vreven, J. A. Montgomery Jr., J. E. Peralta, F. Ogliaro, M. Bearpark, J. J. Heyd, E. Brothers, K. N. Kudin, V. N. Staroverov, R. Kobayashi, J. Normand, K. Raghavachari, A. Rendell, J. C. Burant, S. S. Iyengar, J. Tomasi, M. Cossi, N. Rega, M. J. Millam, M. Klene, J. E. Knox, J. B. Cross, V. Bakken, C. Adamo, J. Jaramillo, R. Gomperts, R. E. Stratmann, O. Yazyev, A. J. Austin, R. Cammi, C. Pomelli, J. W. Ochterski, R. L. Martin, K. Morokuma, V. G. Zakrzewski, G. A. Voth, P. Salvador, J. J. Dannenberg, S. Dapprich, A. D. Daniels, Ö. Farkas, J. B. Foresman, J. V. Ortiz, J. Cioslowski, D. J. Fox, Gaussian 09 (Revision C.01), Gaussian Inc., Wallingford CT, 2009.

47. E. I. Izgorodina, C. Yeh Lin and M. L. Coote, *PCCP*, 2007, **9**, 2507-2516.

48. Y. Zhao and D. Truhlar, *Theor. Chem. Acc.*, 2008, **120**, 215-241.

49. D. J. Henry, M. B. Sullivan and L. Radom, *J. Chem. Phys.*, 2003, **118**, 4849-4860.

50. J. P. Merrick, D. Moran and L. Radom, *J. Phys. Chem. A*, 2007, **111**, 11683-11700.

51. A. V. Marenich, C. J. Cramer and D. G. Truhlar, *J. Phys. Chem. B*, 2009, **113**, 6378-6396.

Chemical Science Accepted Manuscript

52. S. Lecommandoux, F. Chécot, R. Borsali, M. Schappacher, A. Deffieux, A. Brûlet and J. P. Cotton, *Macromolecules*, 2002, **35**, 8878-8881.

53. J. F. J. Coelho, E. Y. Carvalho, D. S. Marques, A. V. Popov, V. Percec and M. H. Gil, *J. Polym. Sci., Part A: Polym. Chem.*, 2008, **46**, 6542-6551.

54. A. P. Haehnel, M. Schneider-Baumann, L. Arens, A. M. Misske, F. Fleischhaker and C. Barner-Kowollik, *Macromolecules*, 2014, **47**, 3483-3496.

55. J. Brandrup and E.-H. Immergut, *Polymer Handbook*, Wiley, Chichester, UK, 1989.

56. T. P. Lodge and M. Muthukumar, *J. Phys. Chem.*, 1996, **100**, 13275-13292.

57. F. Fleischhaker, A. P. Haehnel, A. M. Misske, M. Blanchot, S. Haremza and C. Barner-Kowollik, *Macromol. Chem. Phys.*, 2014, **215**, 1192-1200.

58. M. D. Lechner, E. H. Nordmeier and K. Gehrke, *Makromolekulare Chemie*, Birkhäuser, Basel, 2010.

59. J. M. G. Cown, *Eur. Polym. J.*, 1975, **11**, 297-300.

60. G. M. Martin, S. S. Rogers and L. Mandelkern, *J. Polym. Sci.*, 1956, **20**, 579-581.

61. L. J. Hughes and G. L. Brown, *J. Appl. Polym. Sci.*, 1961, **5**, 580-588.

62. S. Krause, J. J. Gormley, N. Roman, J. A. Shetter and W. H. Watanabe, *J. Polym. Sci. Part A*, 1965, **3**, 3573-3586.

63. J. Heijboer, *Proc. Intern. Conf. on Physics of Non-Crystalline Solids*, North Holland Publishing, Amsterdam, 1965.

64. Z. A. Azimov, S. P. Mitsengendler and A. A. Korotkov, *Polym. Sci. USSR*, 1965, **7**, 929-933.

65. C. E. Rehberg, W. A. Faucette and C. H. Fisher, *J. Am. Chem. Soc.*, 1944, **66**, 1723-1724.

66. J. A. Shetter, *J. Polym. Sci., Part B: Polym. Lett.*, 1963, **1**, 209-213.

67. J. E. Mark, *Physical Properties of Polymers Handbook*, Springer, New York, 2007.